

# Structural Characteristics of Concentrated Aqueous Solutions of Lithium Bromide under Extreme Conditions, Evaluated by the Method of Integral Equations

A. A. Gribkov, M. V. Fedotova, and V. N. Trostin

*Institute of Chemistry of Solutions, Russian Academy of Sciences, Ivanovo, Russia*

Received July 11, 2002

**Abstract**—The influence of temperature ( $T$  298–623 K) at constant pressure ( $P$  200 bar) on the structure of aqueous solutions  $\text{LiBr} : n\text{H}_2\text{O}$  ( $n = 15, 8, 4$ ) was studied using the method of integral equations. In the less concentrated solutions, heating results in disappearance of the tetrahedral ordering of solvent molecules; in the more concentrated solution, this ordering is lacking even at 298 K. In the systems  $\text{LiBr} : 15\text{H}_2\text{O}$  and  $\text{LiBr} : 8\text{H}_2\text{O}$ , with heating, the hydrogen bonding and the coordinating power of the cation get considerably weakened, the amount of contact ion pairs grows, and the amount of hydration-separated ion pairs decreases. On heating, the H bonds between the anion and water molecules of its first coordination sphere are largely ruptured. At the same time, the structuring of the  $\text{LiBr} : 4\text{H}_2\text{O}$  solution under extreme conditions has certain specific features: with increasing temperature, the intermolecular hydrogen bonding becomes stronger, and the amount of hydration-separated ion pairs increases.

Particular attention has been given recently to physicochemical properties of aqueous electrolyte systems under extreme conditions (high temperatures and pressures), owing to development and wide commercial use of new processes involving hydrothermal systems (e.g., hydrothermal oxidation of hazardous chemical wastes, hydrothermal synthesis, hydrothermal processes for recovery of alumina and of nonferrous and heavy metals from the corresponding ores).

The physicochemical properties of liquid-phase systems under both standard and extreme conditions are largely determined by the structural state of the objects and by interparticle interactions in them. Therefore, structuring of such systems is an important field of the modern physical chemistry. Nevertheless, the structural studies at high temperatures and pressures mainly concerned water (see, e.g., [1–14]), whereas structural characteristics of hydrothermal aqueous electrolyte solutions have been studied only in a few works [12, 15–22]. This is due, on the one hand, to the fact that experiments with such systems are difficult and labor-consuming because of high corrosiveness of these systems at elevated temperatures and pressures and of problems with precipitation of the salts, and, on the other hand, to very long computer time required for simulation.

One of the possible ways to derive information on various properties of liquid-phase systems is the method of integral equations, which has been actively used recently to predict the structural characteristics

of aqueous salt solutions under extreme conditions [23–32].

In this work we studied the influence of temperature ( $T$  298–623 K) at constant pressure ( $P$  200 bar) on the structure of concentrated aqueous solutions of  $\text{LiBr}$ ,  $\text{LiBr} : n\text{H}_2\text{O}$  ( $n = 15, 8, 4$ ).

The structural characteristics of these systems were calculated with the Ornstein–Zernicke atom–atom integral equation [33], which in the case of ion-molecular systems is subdivided into three equations describing the solvent–solvent (W–W), ion–solvent (I–W), and ion–ion interactions (I–I):

$$\begin{aligned}\rho_W \hat{h}_{WW}(k) &= \hat{s}_{WW}(k) \hat{c}_{WW}(k) \hat{s}_{WW}(k) \\ &+ \rho_W \hat{s}_{WW}(k) \hat{c}_{WW}(k) \hat{h}_{WW}(k), \\ \hat{h}_{IW}(k) &= \hat{c}_{IW}(k) \hat{s}_{WW}(k) + \rho_W \hat{c}_{IW}(k) \hat{h}_{WW}(k), \\ \hat{h}_{II}(k) &= \hat{c}_{II}(k) + \rho_W \hat{c}_{IW}(k) \hat{h}_{IW}(k) + \rho_I \hat{c}_{II}(k) \hat{h}_{II}(k).\end{aligned}\quad (1)$$

Here  $\rho_W$  is the density of the solvent molecules,  $\rho_I$  is the density of ions, and  $\hat{h}(k)$ ,  $\hat{c}(k)$ , and  $\hat{s}(k)$  are the matrices with the following elements:

$$\begin{aligned}\hat{h}_{\alpha\beta}^{xy}(k) &= \frac{4\pi}{k} (\rho_x \rho_y)^{1/2} \int_0^\infty r dr h_{\alpha\beta}^{xy}(r) \sin(kr), \\ \hat{c}_{\alpha\beta}^{xy}(k) &= \frac{4\pi}{k} (\rho_x \rho_y)^{1/2} \int_0^\infty r dr c_{\alpha\beta}^{xy}(r) \sin(kr), \\ \hat{s}_{\alpha\beta}^{xy}(k) &= \delta_{xy} \left( \delta_{\alpha\beta} + (1 - \delta_{\alpha\beta}) \frac{\sin(kl_{\alpha\beta}^x)}{kl_{\alpha\beta}^x} \right).\end{aligned}$$

**Table 1.** Parameters of the Huggins–Mayer interionic potential

| Parameter                    | Li–Li                  | Li–Br                   | Br–Br                   |
|------------------------------|------------------------|-------------------------|-------------------------|
| $B_{ij}$ , J                 | $7.99 \times 10^{-18}$ | $6.058 \times 10^{-17}$ | $6.135 \times 10^{-16}$ |
| $C_{ij}$ , J nm <sup>6</sup> | $7.3 \times 10^{-27}$  | $2.5 \times 10^{-25}$   | $2.06 \times 10^{-23}$  |
| $\rho_{ij}$ , nm             | 0.0342                 | 0.0353                  | 0.0340                  |

Here  $h_{\alpha\beta}^{xy}(r)$  and  $c_{\alpha\beta}^{xy}(r)$  are the total and direct atom–atom correlation functions of force centers  $\alpha$  and  $\beta$  belonging to particles  $x$  and  $y$ ;  $\hat{s}_{\alpha\beta}^{xy}(r)$  is the Fourier transformant matrix of the function describing intramolecular correlations;  $\rho_x$ , density of particles  $x$ ;  $\rho_y$ , density of particles  $y$ ;  $I_{\alpha\beta}^x$ , intramolecular distance between force centers  $\alpha$  and  $\beta$  belonging to a molecule of kind  $x$ ;  $\delta_{xy}$ , Dirac delta function; and  $\delta_{\alpha\beta}$ , Kronecker delta symbol.

For system of equations (1), we used a hyperchain-type closure:

$$\hat{h}_{\alpha\beta}^{xy} + 1 \equiv g_{\alpha\beta}^{xy}(r) = \exp[-BU_{\alpha\beta}^{xy}(r) + h_{\alpha\beta}^{xy}(r) - c_{\alpha\beta}^{xy}(r)]. \quad (2)$$

Here  $g(r) \equiv g_{\alpha\beta}^{xy}(r)$  is the atom–atom pair correlation function of force centers  $\alpha$  and  $\beta$  belonging to particles  $x$  and  $y$ ;  $U_{\alpha\beta}^{xy}(r) = \Phi_{\alpha\beta}^{xy}(r) + \Phi_{\alpha\beta}^{xy}(r)$  is the initial atom–atom interaction potential (as a sum of short- and long-range constituents);  $b = (k_B T)^{-1}$ , where  $k_B$  is the Boltzmann constant.

For water, we chose the modified SPC (Simple point charge) model [34] with the parameters given in [35]. The short-range interactions between ions and water molecules were described by the Lennard–Jones potential with the parameters taken from [36]. The ion–ion interactions were described by the Huggins–Mayer potential:

$$U_{ij} = q_i q_j / r + B_{ij} \exp(-r/\rho_{ij}) - C_{ij}/r^6. \quad (3)$$

Here  $\theta_i$  is the charge of  $i$ th ion at a distance  $r$  from  $j$ th ion, and the parameters  $B_{ij}$ ,  $C_{ij}$ , and  $\rho_{ij}$  were determined by us from data given in [37] and are presented in Table 1.

Solution of the Ornstein–Zernicke atom–atom equation for the system with a long-range electrostatic interaction potential requires renormalization of the initial long-range potential to obtain an equation including only the renormalized long-range interaction potential, so-called shielded potential. The scheme of this procedure and the method for numerical solution of the Ornstein–Zernicke atom–atom equation in the hyperchain approximation are described in detail elsewhere [38].

Calculations gave for the lithium bromide solutions under consideration the pair correlation functions  $g_{\alpha\beta}(r)$  from which we determined the interparticle distances and the presence and kind of ionic associates in solutions. Also, we calculated the coordination numbers of particles:

$$n_{\alpha\beta} = 4\pi\rho_{\beta} \int_0^{r_{m1}} g_{\alpha\beta}(r)r^2 dr. \quad (4)$$

Here  $\rho_{\beta}$  is the density of particles of kind  $\beta$  ( $\text{\AA}^{-3}$ ), and  $r_{m1}$ , position of the first minimum in the pair correlation function  $g_{\alpha\beta}(r)$ . From the relative variation of  $\Delta n_{\alpha\beta}(r_{m1})$ , we analyzed changes in the structural parameters of the solvent and the associative and coordinative powers of ions depending on the external conditions:

$$\Delta n_{\alpha\beta}(r_{m1}) = \frac{n_{\alpha\beta}^T(r_{m1}) - n_{\alpha\beta}^{298}(r_{m1})}{n_{\alpha\beta}^{298}(r_{m1})} \times 100\%. \quad (5)$$

Here  $n_{\alpha\beta}^T(r_{m1})$  is the coordination number of a particle at a temperature differing from the standard temperature.

The characteristic values of the calculated functions throughout the temperature range studied are given in Tables 2–4. The functions  $g_{\alpha\beta}(r)$  and  $n_{\alpha\beta}(r)$  for 298 and 623 K are plotted as examples in Figs. 1–3.

**Water–water (W–W) correlations.** As seen from our results (Tables 2–4, Fig. 1), heating of the solutions results in that the major peak of the function  $g_{O-O}(r)$ , determined by interactions of water molecules in the unbound solvent, considerably decreases in the intensity. The position of the first maximum remains unchanged. With the LiBr:4H<sub>2</sub>O system, the first minimum of this correlation function shifts toward longer distances and decreases in depth. As a result, the quantity  $n_{O-O}^{(I)}(r_{m1})$ , determining the number of water molecules that are the nearest neighbors, increases (by 17.9%) with temperature. Similar trends are observed in less concentrated solutions also, but only in the range 298–373 K. The quantity  $n_{O-O}^{(I)}(r_{m1})$  grows in this range by 2.2% for the LiBr:8H<sub>2</sub>O system and by 2.7% for the LiBr:15H<sub>2</sub>O system (Fig. 4). Further heating results in disappearance of the first minimum (Tables 2, 3).

According to experimental structural studies (see, e.g., [39–42]), the radial distribution function for water has a peak at a distance of 0.44–0.45 nm, determining the tetrahedral structure of water. As seen from Tables 2 and 3, at standard temperature the pair correlation functions  $g_{O-O}(r)$  for the LiBr:15H<sub>2</sub>O and LiBr:8H<sub>2</sub>O systems have a peak at 0.428 and 0.434 nm, respectively. This peak decreases in inten-

**Table 2.** Characteristic values of some structural parameters for the system LiBr:15H<sub>2</sub>O under conditions of heating ( $T$  298–623 K,  $P$  200 bar)<sup>a</sup>

| Parameter           | 298 K          | 323 K          | 373 K          | 423 K          |
|---------------------|----------------|----------------|----------------|----------------|
| $g_{O-O}(r_{M1})$   | 3.009 (0.292)  | 2.916 (0.292)  | 2.757 (0.290)  | 2.615 (0.290)  |
| $g_{O-O}(r_{m1})$   | 0.886 (0.396)  | 0.886 (0.398)  | 0.889 (0.406)  | –              |
| $g_{O-O}(r_{M2})$   | 0.898 (0.428)  | 0.894 (0.428)  | 0.891 (0.428)  | –              |
| $g_{O-O}(r_{m1})$   | 0.871 (0.480)  | 0.874 (0.478)  | 0.879 (0.474)  | 0.885 (0.470)  |
| $g_{O-H}(r_{M1})$   | 1.927 (0.146)  | 1.826 (0.146)  | 1.670 (0.144)  | 1.566 (0.144)  |
| $g_{O-H}(r_{m1})$   | 0.097 (0.194)  | 0.111 (0.194)  | 0.138 (0.194)  | 0.161 (0.194)  |
| $g_{Li-O}(r_{M1})$  | 12.910 (0.190) | 12.222 (0.190) | 10.974 (0.190) | 9.879 (0.190)  |
| $g_{Li-O}(r_{m1})$  | 0.050 (0.258)  | 0.061 (0.260)  | 0.081 (0.260)  | 0.099 (0.262)  |
| $g_{Li-H}(r_{M1})$  | 2.054 (0.268)  | 1.994 (0.268)  | 1.879 (0.270)  | 1.769 (0.272)  |
| $g_{Li-H}(r_{m1})$  | 0.676 (0.352)  | 0.689 (0.352)  | 0.711 (0.350)  | 0.727 (0.350)  |
| $g_{Br-O}(r_{M1})$  | 2.551 (0.356)  | 2.550 (0.354)  | 2.513 (0.354)  | 2.440 (0.354)  |
| $g_{Br-O}(r_{m1})$  | 0.804 (0.450)  | 0.813 (0.454)  | 0.820 (0.462)  | 0.819 (0.470)  |
| $g_{Br-H}(r_{M1})$  | 4.033 (0.204)  | 3.767 (0.202)  | 3.285 (0.202)  | 2.866 (0.202)  |
| $g_{Br-H}(r_{m1})$  | 0.247 (0.268)  | 0.269 (0.268)  | 0.304 (0.268)  | 0.327 (0.268)  |
| $g_{Li-Br}(r_{M1})$ | 1.414 (0.252)  | 2.222 (0.250)  | 4.363 (0.246)  | 6.718 (0.244)  |
| $g_{Li-Br}(r_{m1})$ | 0.553 (0.314)  | 0.698 (0.318)  | 0.943 (0.328)  | 1.091 (0.336)  |
| $g_{Li-Br}(r_{M2})$ | 3.299 (0.444)  | 3.092 (0.444)  | 2.698 (0.446)  | 2.340 (0.448)  |
| $g_{Li-Br}(r_{m2})$ | 1.006 (0.606)  | 0.987 (0.612)  | 0.962 (0.624)  | 0.949 (0.638)  |
| Parameter           | 473 K          | 523 K          | 573 K          | 623 K          |
| $g_{O-O}(r_{M1})$   | 2.484 (0.290)  | 2.362 (0.292)  | 2.245 (0.292)  | 2.141 (0.292)  |
| $g_{O-O}(r_{m1})$   | –              | –              | –              | –              |
| $g_{O-O}(r_{M2})$   | –              | –              | –              | –              |
| $g_{O-O}(r_{m1})$   | 0.892 (0.470)  | 0.901 (0.470)  | 0.906 (0.470)  | 0.916 (0.470)  |
| $g_{O-H}(r_{M1})$   | 1.486 (0.144)  | 1.427 (0.144)  | 1.376 (0.144)  | 1.340 (0.144)  |
| $g_{O-H}(r_{m1})$   | 0.180 (0.196)  | 0.196 (0.196)  | 0.210 (0.196)  | 0.221 (0.196)  |
| $g_{Li-O}(r_{M1})$  | 9.082 (0.188)  | 8.441 (0.188)  | 8.099 (0.188)  | 7.752 (0.188)  |
| $g_{Li-O}(r_{m1})$  | 0.115 (0.262)  | 0.130 (0.264)  | 0.152 (0.266)  | 0.166 (0.266)  |
| $g_{Li-H}(r_{M1})$  | 1.676 (0.272)  | 1.598 (0.272)  | 1.570 (0.272)  | 1.526 (0.272)  |
| $g_{Li-H}(r_{m1})$  | 0.738 (0.350)  | 0.745 (0.350)  | 0.768 (0.348)  | 0.770 (0.348)  |
| $g_{Br-O}(r_{M1})$  | 2.352 (0.356)  | 2.258 (0.356)  | 2.249 (0.356)  | 2.156 (0.358)  |
| $g_{Br-O}(r_{m1})$  | 0.819 (0.476)  | 0.821 (0.480)  | 0.862 (0.486)  | 0.869 (0.490)  |
| $g_{Br-H}(r_{M1})$  | 2.539 (0.202)  | 2.286 (0.202)  | 2.134 (0.202)  | 2.001 (0.200)  |
| $g_{Br-H}(r_{m1})$  | 0.342 (0.268)  | 0.351 (0.268)  | 0.365 (0.268)  | 0.368 (0.268)  |
| $g_{Li-Br}(r_{M1})$ | 9.032 (0.242)  | 11.188 (0.240) | 12.422 (0.238) | 14.657 (0.238) |
| $g_{Li-Br}(r_{m1})$ | 1.160 (0.344)  | 1.180 (0.352)  | 0.985 (0.362)  | 0.947 (0.370)  |
| $g_{Li-Br}(r_{M2})$ | 2.052 (0.452)  | 1.837 (0.458)  | 1.291 (0.454)  | 1.162 (0.462)  |
| $g_{Li-Br}(r_{m2})$ | 0.949 (0.648)  | 0.962 (0.658)  | 0.693 (0.652)  | 0.695 (0.660)  |

<sup>a</sup> ( $r_{Mi}$ ) Position of  $i$ th maximum and ( $r_{mi}$ ) position of  $i$ th minimum (nm, given in parentheses). The same for Tables 3 and 4.

sity on heating to 373 K. The second minimum of the  $g_{O-O}(r)$  function shifts toward shorter distances and decreases in the depth. As a result, the number of tetrahedrally ordered water molecules  $n_{O-O}^{(II)}(r_{m2})$  decreases (in the range 298–373 K, by 21.1% with the LiBr: 15H<sub>2</sub>O system and by 27.4% with the LiBr: 8H<sub>2</sub>O system) (Fig. 4). A part of these water molecules become the nearest neighbors, which explains

the growth of  $n_{O-O}^{(I)}(r_{m1})$ . As already noted, further heating causes disappearance of the first minimum of the pair correlation function  $g_{O-O}(r)$ , with the second peak transforming into a long plateau (Fig. 1). Since at  $T > 373$  K the first minimum of the function is lacking, it seems impossible to separate the interactions between the nearest water molecules and between water molecules arranged in the points of its

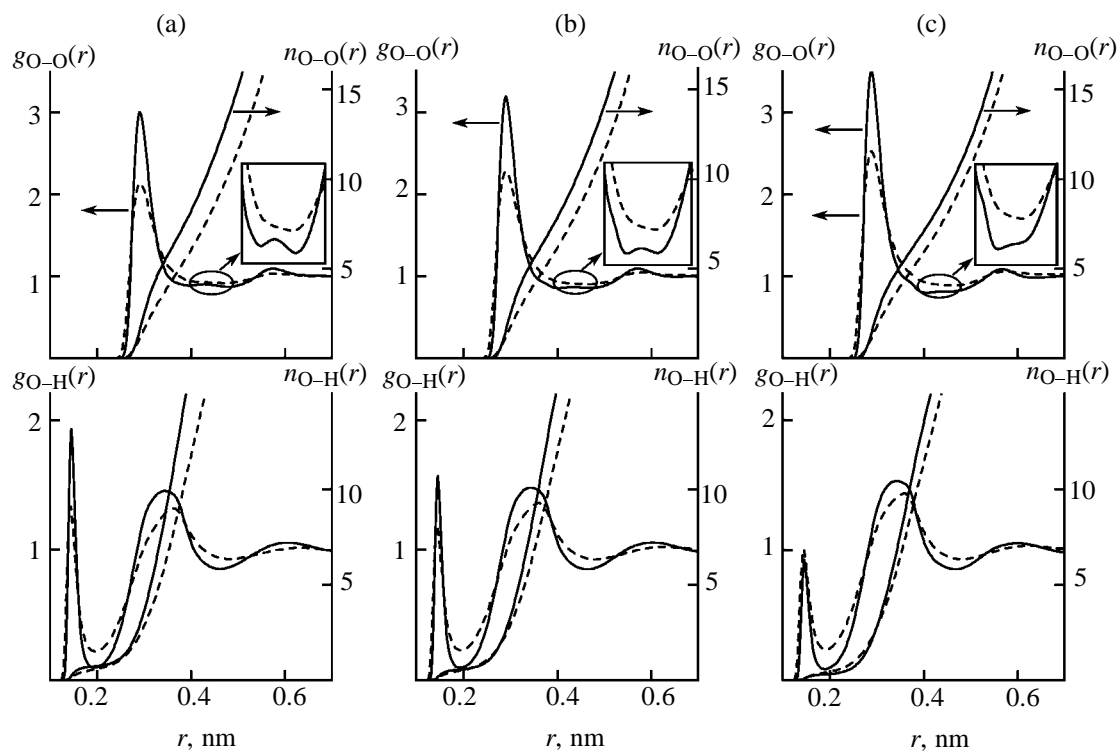


**Fig. 1.** Pair correlation functions  $g_{W-W}(r)$  and number of interactions  $n_{W-W}(r)$  for solutions (a) LiBr:15H<sub>2</sub>O, (b) LiBr:8H<sub>2</sub>O, and (c) LiBr:4H<sub>2</sub>O at 200 bar and (solid line) 298 and (dashed line) 623 K.

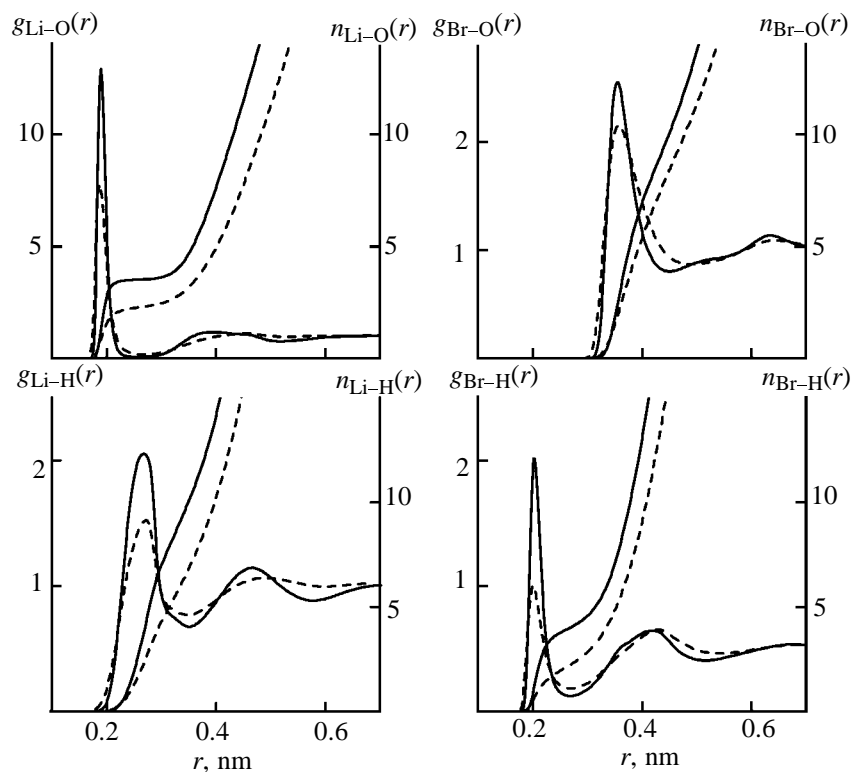


**Fig. 2.** Pair correlation functions  $g_{I-W}(r)$  and number of interactions  $n_{I-W}(r)$  for LiBr:15H<sub>2</sub>O solution at 200 bar and (solid line) 298 and (dashed line) 623 K.

**Table 3.** Characteristic values of some structural parameters for the system LiBr:8H<sub>2</sub>O under conditions of heating (*T* 298–623 K, *P* 200 bar)

| Parameter                  | 298 K          | 323 K          | 373 K          | 423 K          |
|----------------------------|----------------|----------------|----------------|----------------|
| $g_{\text{O-O}}(r_{M1})$   | 3.197 (0.290)  | 3.094 (0.290)  | 2.913 (0.290)  | 2.725 (0.290)  |
| $g_{\text{O-O}}(r_{m1})$   | 0.854 (0.402)  | 0.856 (0.404)  | 0.864 (0.412)  | –              |
| $g_{\text{O-O}}(r_{M2})$   | 0.864 (0.434)  | 0.863 (0.434)  | 0.865 (0.434)  | –              |
| $g_{\text{O-O}}(r_{m1})$   | 0.855 (0.472)  | 0.857 (0.468)  | 0.862 (0.464)  | 0.866 (0.462)  |
| $g_{\text{O-H}}(r_{M1})$   | 1.569 (0.146)  | 1.507 (0.146)  | 1.419 (0.146)  | 1.360 (0.144)  |
| $g_{\text{O-H}}(r_{m1})$   | 0.096 (0.194)  | 0.111 (0.194)  | 0.138 (0.194)  | 0.159 (0.194)  |
| $g_{\text{Li-O}}(r_{M1})$  | 13.364 (0.190) | 12.532 (0.190) | 11.012 (0.190) | 10.042 (0.188) |
| $g_{\text{Li-O}}(r_{m1})$  | 0.048 (0.258)  | 0.058 (0.260)  | 0.075 (0.260)  | 0.094 (0.262)  |
| $g_{\text{Li-H}}(r_{M1})$  | 2.150 (0.270)  | 2.075 (0.270)  | 1.925 (0.272)  | 1.833 (0.272)  |
| $g_{\text{Li-H}}(r_{m1})$  | 0.708 (0.352)  | 0.719 (0.352)  | 0.737 (0.352)  | 0.768 (0.350)  |
| $g_{\text{Br-O}}(r_{M1})$  | 2.603 (0.354)  | 2.597 (0.354)  | 2.543 (0.354)  | 2.553 (0.354)  |
| $g_{\text{Br-O}}(r_{m1})$  | 0.810 (0.452)  | 0.812 (0.456)  | 0.805 (0.466)  | 0.835 (0.472)  |
| $g_{\text{Br-H}}(r_{M1})$  | 4.254 (0.204)  | 3.912 (0.202)  | 3.302 (0.202)  | 2.860 (0.202)  |
| $g_{\text{Br-H}}(r_{m1})$  | 0.264 (0.268)  | 0.285 (0.268)  | 0.317 (0.268)  | 0.342 (0.268)  |
| $g_{\text{Li-Br}}(r_{M1})$ | 1.892 (0.250)  | 2.749 (0.248)  | 4.494 (0.246)  | 5.842 (0.244)  |
| $g_{\text{Li-Br}}(r_{m1})$ | 0.541 (0.318)  | 0.646 (0.324)  | 0.795 (0.332)  | 0.793 (0.340)  |
| $g_{\text{Li-Br}}(r_{M2})$ | 2.545 (0.444)  | 2.386 (0.446)  | 2.082 (0.448)  | 1.599 (0.450)  |
| $g_{\text{Li-Br}}(r_{m2})$ | 0.866 (0.600)  | 0.869 (0.604)  | 0.881 (0.618)  | 0.724 (0.632)  |
| Parameter                  | 473 K          | 523 K          | 573 K          | 623 K          |
| $g_{\text{O-O}}(r_{M1})$   | 2.614 (0.290)  | 2.491 (0.290)  | 2.387 (0.290)  | 2.289 (0.290)  |
| $g_{\text{O-O}}(r_{m1})$   | –              | –              | –              | –              |
| $g_{\text{O-O}}(r_{M2})$   | –              | –              | –              | –              |
| $g_{\text{O-O}}(r_{m1})$   | 0.870 (0.458)  | 0.878 (0.460)  | 0.894 (0.464)  | 0.903 (0.466)  |
| $g_{\text{O-H}}(r_{M1})$   | 1.296 (0.144)  | 1.252 (0.144)  | 1.227 (0.144)  | 1.192 (0.144)  |
| $g_{\text{O-H}}(r_{m1})$   | 0.182 (0.194)  | 0.200 (0.194)  | 0.215 (0.194)  | 0.229 (0.194)  |
| $g_{\text{Li-O}}(r_{M1})$  | 9.042 (0.188)  | 8.320 (0.188)  | 7.584 (0.188)  | 7.102 (0.188)  |
| $g_{\text{Li-O}}(r_{m1})$  | 0.112 (0.262)  | 0.128 (0.264)  | 0.136 (0.266)  | 0.150 (0.266)  |
| $g_{\text{Li-H}}(r_{M1})$  | 1.719 (0.272)  | 1.630 (0.274)  | 1.516 (0.272)  | 1.453 (0.272)  |
| $g_{\text{Li-H}}(r_{m1})$  | 0.779 (0.350)  | 0.784 (0.350)  | 0.761 (0.350)  | 0.760 (0.350)  |
| $g_{\text{Br-O}}(r_{M1})$  | 2.476 (0.354)  | 2.390 (0.354)  | 2.209 (0.356)  | 2.128 (0.356)  |
| $g_{\text{Br-O}}(r_{m1})$  | 0.826 (0.476)  | 0.827 (0.480)  | 0.791 (0.484)  | 0.793 (0.486)  |
| $g_{\text{Br-H}}(r_{M1})$  | 2.481 (0.202)  | 2.204 (0.202)  | 1.957 (0.202)  | 1.793 (0.202)  |
| $g_{\text{Br-H}}(r_{m1})$  | 0.363 (0.268)  | 0.374 (0.268)  | 0.370 (0.268)  | 0.375 (0.268)  |
| $g_{\text{Li-Br}}(r_{M1})$ | 6.973 (0.242)  | 7.976 (0.240)  | 9.319 (0.240)  | 10.242 (0.238) |
| $g_{\text{Li-Br}}(r_{m1})$ | 0.827 (0.346)  | 0.828 (0.352)  | 0.924 (0.356)  | 0.925 (0.362)  |
| $g_{\text{Li-Br}}(r_{M2})$ | 1.422 (0.454)  | 1.279 (0.462)  | 1.428 (0.488)  | 1.392 (0.504)  |
| $g_{\text{Li-Br}}(r_{m2})$ | 0.733 (0.640)  | 0.740 (0.646)  | 0.953 (0.666)  | 0.978 (0.682)  |

tetrahedral structure. In this case, structural changes in solution can be judged from variation of  $n_{\text{O-O}}^{(\text{I+II})}(r_{m2})$ , which is the sum of  $n_{\text{O-O}}^{(\text{I})}(r_{m1})$  and  $n_{\text{O-O}}^{(\text{II})}(r_{m2})$ . In the range 373–623 K, this quantity decreases by 23% for the LiBr:15H<sub>2</sub>O system and by 14.7% for the LiBr:8H<sub>2</sub>O system (Fig. 4).

In the case of the LiBr:4H<sub>2</sub>O solution, the peak in the pair correlation function  $g_{\text{O-O}}(r)$  corresponding to

the tetrahedral structure of water is absent even at standard temperature, suggesting total absence of tetrahedral ordering of water molecules, which is typical of highly concentrated solutions.

As the temperature increases, the major peak of the pair correlation function  $g_{\text{O-H}}(r)$  for the systems LiBr:15H<sub>2</sub>O and LiBr:8H<sub>2</sub>O considerably decreases in intensity and gets broadened. Simultaneously, the first

**Table 4.** Characteristic values of some structural parameters for the system LiBr:4H<sub>2</sub>O under conditions of heating ( $T$  298–623 K,  $P$  200 bar)

| Parameter           | 298 K          | 323 K          | 373 K          | 423 K         |
|---------------------|----------------|----------------|----------------|---------------|
| $g_{O-O}(r_{M1})$   | 3.512 (0.288)  | 3.391 (0.288)  | 3.187 (0.288)  | 3.020 (0.288) |
| $g_{O-O}(r_{m1})$   | 0.797 (0.406)  | 0.809 (0.408)  | 0.828 (0.416)  | 0.846 (0.442) |
| $g_{O-H}(r_{M1})$   | 0.923 (0.146)  | 0.967 (0.146)  | 1.012 (0.146)  | 1.039 (0.146) |
| $g_{O-H}(r_{m1})$   | 0.087 (0.190)  | 0.102 (0.190)  | 0.133 (0.190)  | 0.160 (0.190) |
| $g_{Li-O}(r_{M1})$  | 13.675 (0.190) | 12.561 (0.190) | 10.831 (0.188) | 9.515 (0.188) |
| $g_{Li-O}(r_{m1})$  | 0.041 (0.258)  | 0.048 (0.260)  | 0.063 (0.260)  | 0.077 (0.262) |
| $g_{Li-H}(r_{M1})$  | 2.231 (0.272)  | 2.126 (0.272)  | 1.946 (0.272)  | 1.788 (0.272) |
| $g_{Li-H}(r_{m1})$  | 0.754 (0.350)  | 0.761 (0.352)  | 0.768 (0.352)  | 0.769 (0.352) |
| $g_{Br-O}(r_{M1})$  | 2.724 (0.354)  | 2.683 (0.354)  | 2.595 (0.354)  | 2.491 (0.354) |
| $g_{Br-O}(r_{m1})$  | 0.806 (0.462)  | 0.790 (0.464)  | 0.766 (0.470)  | 0.748 (0.474) |
| $g_{Br-H}(r_{M1})$  | 4.364 (0.204)  | 3.887 (0.204)  | 3.177 (0.202)  | 2.637 (0.202) |
| $g_{Br-H}(r_{m1})$  | 0.285 (0.268)  | 0.302 (0.268)  | 0.332 (0.268)  | 0.350 (0.268) |
| $g_{Li-Br}(r_{M1})$ | 4.008 (0.246)  | 4.576 (0.246)  | 5.679 (0.244)  | 6.154 (0.242) |
| $g_{Li-Br}(r_{m1})$ | 0.581 (0.330)  | 0.625 (0.332)  | 0.688 (0.338)  | 0.718 (0.344) |
| $g_{Li-Br}(r_{M2})$ | 1.929 (0.448)  | 1.794 (0.450)  | 1.586 (0.456)  | 1.442 (0.464) |
| $g_{Li-Br}(r_{m2})$ | 0.816 (0.594)  | 0.838 (0.600)  | 0.868 (0.642)  | 0.889 (0.654) |
| Parameter           | 473 K          | 523 K          | 573 K          | 623 K         |
| $g_{O-O}(r_{M1})$   | 2.877 (0.288)  | 2.745 (0.288)  | 2.627 (0.288)  | 2.522 (0.288) |
| $g_{O-O}(r_{m1})$   | 0.858 (0.452)  | 0.868 (0.458)  | 0.879 (0.460)  | 0.888 (0.462) |
| $g_{O-H}(r_{M1})$   | 1.039 (0.146)  | 1.029 (0.144)  | 1.018 (0.144)  | 1.003 (0.144) |
| $g_{O-H}(r_{m1})$   | 0.184 (0.190)  | 0.204 (0.192)  | 0.222 (0.192)  | 0.237 (0.192) |
| $g_{Li-O}(r_{M1})$  | 8.529 (0.188)  | 7.765 (0.188)  | 7.129 (0.188)  | 6.612 (0.188) |
| $g_{Li-O}(r_{m1})$  | 0.092 (0.264)  | 0.107 (0.264)  | 0.122 (0.264)  | 0.136 (0.266) |
| $g_{Li-H}(r_{M1})$  | 1.665 (0.274)  | 1.568 (0.274)  | 1.485 (0.274)  | 1.417 (0.274) |
| $g_{Li-H}(r_{m1})$  | 0.770 (0.352)  | 0.769 (0.352)  | 0.767 (0.352)  | 0.766 (0.352) |
| $g_{Br-O}(r_{M1})$  | 2.398 (0.354)  | 2.314 (0.354)  | 2.232 (0.354)  | 2.157 (0.354) |
| $g_{Br-O}(r_{m1})$  | 0.740 (0.476)  | 0.738 (0.480)  | 0.739 (0.482)  | 0.742 (0.484) |
| $g_{Br-H}(r_{M1})$  | 2.254 (0.202)  | 1.991 (0.202)  | 1.777 (0.202)  | 1.611 (0.202) |
| $g_{Br-H}(r_{m1})$  | 0.365 (0.268)  | 0.376 (0.268)  | 0.383 (0.268)  | 0.388 (0.268) |
| $g_{Li-Br}(r_{M1})$ | 6.597 (0.242)  | 7.067 (0.240)  | 7.277 (0.240)  | 7.450 (0.240) |
| $g_{Li-Br}(r_{m1})$ | 0.736 (0.348)  | 0.744 (0.354)  | 0.748 (0.358)  | 0.750 (0.362) |
| $g_{Li-Br}(r_{M2})$ | 1.352 (0.480)  | 1.307 (0.502)  | 1.285 (0.510)  | 1.271 (0.514) |
| $g_{Li-Br}(r_{m2})$ | 0.912 (0.662)  | 0.933 (0.670)  | 0.951 (0.680)  | 0.964 (0.692) |

minimum noticeably decreases in the depth (Fig. 1; Tables 2, 3). As a result, the number of intermolecular hydrogen bonds  $n_{O-H}$  decreases, which is consistent with the results of both experimental studies [11, 43–45] and computer simulation [6, 7, 46] of pure water under subcritical and supercritical conditions. In the LiBr:15H<sub>2</sub>O system,  $n_{O-H}(r_{m1})$  decreased by 20.4%, and in the LiBr:8H<sub>2</sub>O system, by 8.3% (Fig. 4).

For the most concentrated solution, the height of the major peak at  $T$  298 K is considerably smaller than for the more dilute solutions (Fig. 1), suggesting lower probability of formation of hydrogen bonds in

the LiBr:4H<sub>2</sub>O solution. As the temperature is increased to 473 K, the first peak of the  $g_{O-H}(r)$  function slightly grows in intensity, and on further heating it starts to decrease. The other functional changes are similar to those occurring in less concentrated systems. As a result,  $n_{O-H}(r_{m1})$  increases from 0.302 at 298 K to 0.409 at 573 K, slightly decreasing on further heating to 623 K (0.406; overall growth 34.4%) (Fig. 4). Such enhancement of hydrogen bonding with temperature was observed previously in our studies of highly concentrated LiCl solutions, LiCl:3H<sub>2</sub>O [27].

**Ion–water (I–W) correlations.** Figure 2 shows the

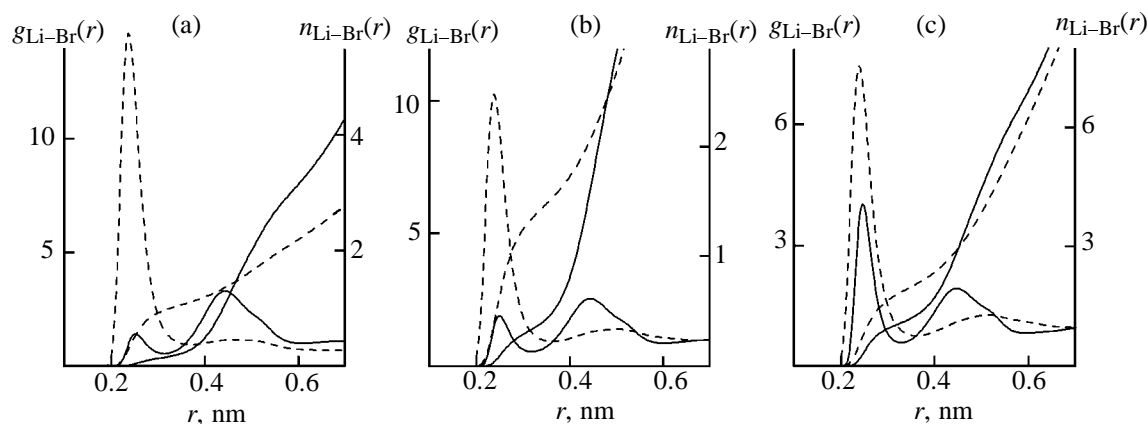


**Fig. 3.** Pair correlation functions  $g_{\text{Li-Br}}(r)$  and number of interactions  $n_{\text{Li-Br}}(r)$  for solutions (a) LiBr:15H<sub>2</sub>O, (b) LiBr:8H<sub>2</sub>O, and (c) LiBr:4H<sub>2</sub>O at 200 bar and (solid line) 298 and (dashed line) 623 K.

pair correlation functions  $g_{\text{Li-O}}(r)$ ,  $g_{\text{Li-H}}(r)$ ,  $g_{\text{Br-O}}(r)$ , and  $g_{\text{Br-H}}(r)$  for the LiBr:15H<sub>2</sub>O system as example. For the LiBr:8H<sub>2</sub>O and LiBr:4H<sub>2</sub>O solutions, the functions and the trends in their variation with temperature are similar.

Under standard conditions, the  $g_{\text{Li-O}}(r)$  function for all the three solutions has a peak at a distance of 0.190 nm, determined by interactions between the Li<sup>+</sup> ion and water molecules in its nearest surrounding. This is consistent with the majority of experimental structural data for lithium systems (see, e.g., [47–50]).

With increasing temperature, irrespective of the solution concentration, the major peak of the pair correlation function  $g_{\text{Li-O}}(r)$  appreciably decreases in the intensity, and its maximum slightly shifts toward shorter  $r$ . Also, the first minimum decreases in the depth and shifts toward longer distances (Fig. 2). As a result, the number of water molecules in the first coordination sphere of the Li<sup>+</sup> ion appreciably decreases (Tables 2–4). In particular,  $n_{\text{Li-O}}(r_{m1})$  decreases by 34.4% in the LiBr:15H<sub>2</sub>O system, by 38.1% in the LiBr:8H<sub>2</sub>O system, and by 40.4% in the LiBr:4H<sub>2</sub>O system (Fig. 4), suggesting thermal dehydration of the cation accompanied by shortening of the  $r_{\text{Li}^+-\text{O}}$  distance.

In the  $g_{\text{Li-H}}(r)$  function, the intensity of the major peak and the depth of the first minimum also noticeably decrease with temperature (Fig. 2). As a result, the number of Li–H<sup>+</sup> interactions considerably decreases: by 34.2% in the LiBr:15H<sub>2</sub>O system, by 33.6% in the LiBr:8H<sub>2</sub>O system, and by 31.1% in the LiBr:4H<sub>2</sub>O system (Tables 2–4, Fig. 4).

The results obtained show that, on heating, the coordinative power of the Li<sup>+</sup> ion appreciably weak-

ens, and the ordering of water molecules in its first hydration sphere decreases.

Under standard conditions, the pair correlation functions  $g_{\text{Br-O}}(r)$  have the major peak at a distance of 0.354 nm, determined by interactions (strong hydrogen bonding) of the anion with the oxygen atoms of water molecules. This distance somewhat exceeds the distance found for bromide systems in some X-ray diffraction studies. The experimental value varies from 0.329 to 0.343 nm depending on solution concentration (see, e.g., [51–55]).

The intensity of the major peak of the pair correlation function  $g_{\text{Br-O}}(r)$  appreciably decreases with increasing temperature, irrespective of the solution concentration. With the LiBr:15H<sub>2</sub>O system, the depth of the first minimum decreases with increasing temperature, whereas with more concentrated solutions (LiBr:8H<sub>2</sub>O and LiBr:4H<sub>2</sub>O) it, on the contrary, increases. The first minimum of this function shifts toward longer distances with temperature for all the three systems. The  $n_{\text{Br-O}}(r_{m1})$ – $T$  diagrams (Fig. 4) show that, in less concentrated solutions, the coordinative power of the bromide ion increases on heating to 473 K and decreases at higher temperatures. With the LiBr:4H<sub>2</sub>O solution, the trend is similar but the maximum is observed at 373 K. On the whole, the number of Br<sup>–</sup>–O interactions increases with temperature by 6.7% in the LiBr:15H<sub>2</sub>O system and by 2.5% in the LiBr:8H<sub>2</sub>O system. In the LiBr:4H<sub>2</sub>O system, however,  $n_{\text{Br-O}}(r_{m1})$  decreases by 6% in going from 298 to 623 K, suggesting dehydration of the anion and weakening of its coordinative power in the highly concentrated solution.

The influence of temperature on the pair correlation function  $g_{\text{Br-H}}(r)$  is more pronounced. Irrespective

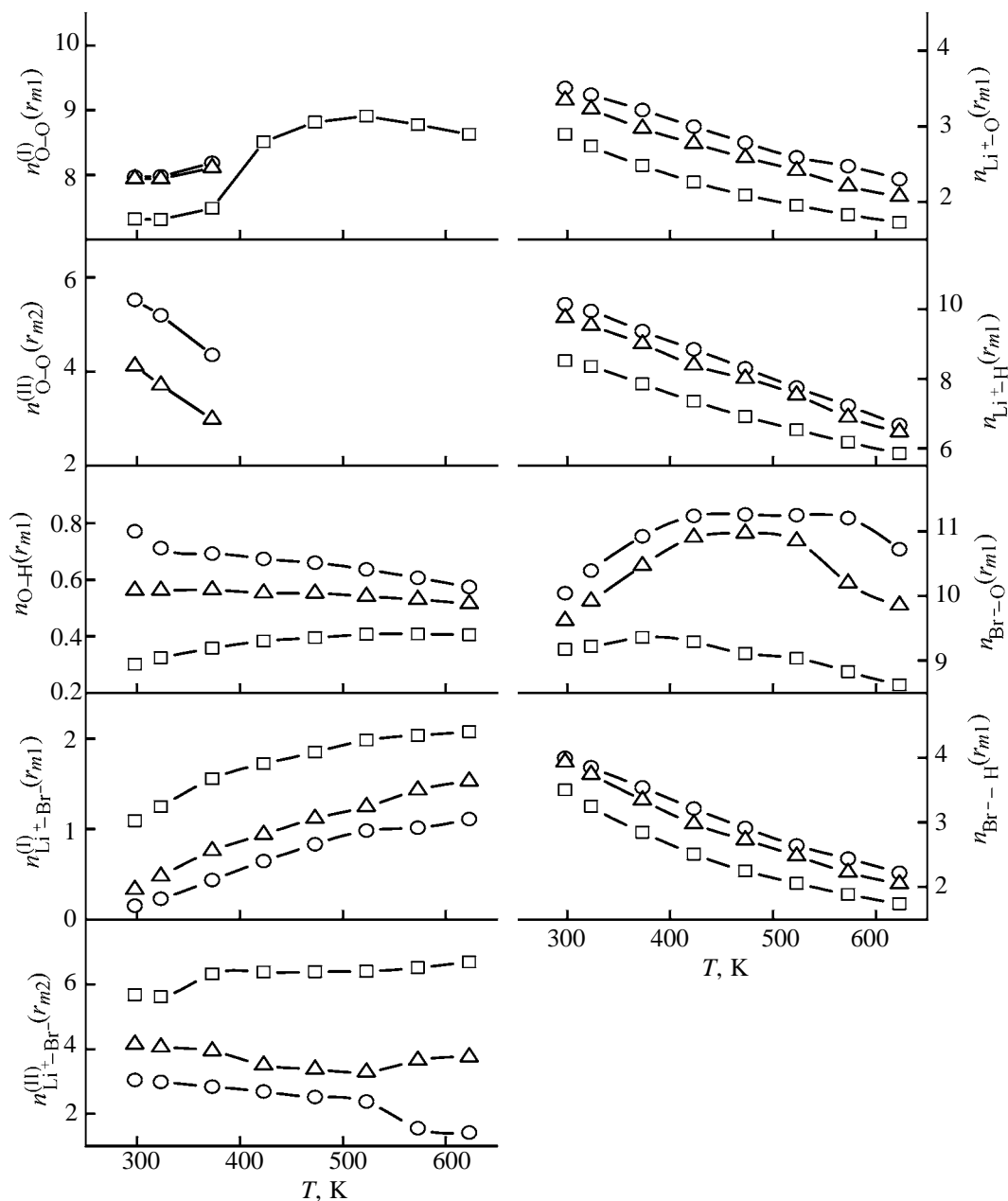


**Fig. 4.** Temperature dependence of the coordination numbers of particles in solutions (circles) LiBr:15H<sub>2</sub>O, (triangles) LiBr:8H<sub>2</sub>O, and (squares) LiBr:4H<sub>2</sub>O.

of the solution concentration, the major peak of the  $g_{\text{Br-H}}(r)$  function appreciably decreases in the intensity on heating (Fig. 2). The positions of the first maximum and first minimum remain virtually unchanged; only the depth of the minimum decreases (Tables 2–4). In all the three systems, heating is accompanied by a decrease in the number of Br<sup>−</sup>–H bonds (by 44.5% in the LiBr:15H<sub>2</sub>O system, by 47.9% in the LiBr:8H<sub>2</sub>O system, and by 50.2% in the LiBr:4H<sub>2</sub>O system) (Fig. 4), which illustrates exten-

sive rupture of hydrogen bonds between the anion and the water molecules of its first hydration sphere.

Thus, comparison of the relative changes in the number of water molecules in the first coordination spheres of the Li<sup>+</sup> and Br<sup>−</sup> ions shows that isobaric heating in these systems affects more strongly the coordinative power of the Li<sup>+</sup> ion ( $\Delta n_{\text{Li-O}}(r_{m1}) > \Delta n_{\text{Br-O}}(r_{m1})$ ).

**Ion-ion (I–I) correlations.** Under standard condi-



tions, the pair correlation functions  $g_{\text{Li-Br}}(r)$  for the LiBr:15H<sub>2</sub>O, LiBr:8H<sub>2</sub>O, and LiBr:4H<sub>2</sub>O solutions have the major peak at distances of 0.252, 0.250, and 0.246 nm, respectively; this peak is due to the Li<sup>+</sup>–Br<sup>−</sup> contact interactions (Fig. 3). In the most concentrated solution, this peak is the strongest. The second peak of the  $g_{\text{Li-Br}}(r)$  function is also well resolved at the standard parameters of state; this peak is due to the presence in solution of hydration-separated ion pairs Li<sup>+</sup>⋯H<sub>2</sub>O⋯Br<sup>−</sup>. With increasing temperature, the major peak appreciably grows in intensity, and the first maximum shifts toward shorter  $r$  (Tables 2–4). The first minimum decreases in the depth and shifts toward longer  $r$ . Thus, the amount of contact ion pairs noticeably grows with temperature (Fig. 4), with the changes in  $n_{\text{Li-Br}}^{(\text{I})}(r_{m1})$  being the stronger, the lower the solution concentration. In particular, the amount of contact ion pairs increased by a factor of 7.4 in the LiBr:15H<sub>2</sub>O system, by a factor of 4.6 in the LiBr:8H<sub>2</sub>O system, and by a factor of 1.9 in the LiBr:4H<sub>2</sub>O system.

The second peak determined by interaction of lithium and bromide ions in the Li<sup>+</sup>⋯H<sub>2</sub>O⋯Br<sup>−</sup> chains appreciably decreases with increasing temperature, irrespective of the solution concentration (Fig. 3). The second maximum and second minimum shift toward longer distances. The second minimum increases in the depth for the LiBr:15H<sub>2</sub>O solution and decreases for the more concentrated solutions. As a result, the amount of hydration-separated ion pairs decreases by a factor of 2.1 in the LiBr:15H<sub>2</sub>O solution and by a factor of 1.1 in the LiBr:8H<sub>2</sub>O solution (Fig. 4).

In the case of the LiBr:4H<sub>2</sub>O system, the quantity  $n_{\text{Li-Br}}^{(\text{II})}(r_{m2})$  increases on heating by 17.9%. Such features of structuring of the highly concentrated LiBr solution may be due to formation of a melt-like bond system [32, 43, 56].

Comparison of changes in the amounts of contact and hydration-separated ion pairs shows that heating exerts a stronger effect on the former quantity, irrespective of the solution concentration.

Thus, heating will appreciably affect formation of the structure of concentrated aqueous solutions of lithium bromide. Our results show that the structuring of the LiBr:15H<sub>2</sub>O and LiBr:8H<sub>2</sub>O solutions is similar to structuring of the majority of hydrothermal systems [43, 56]. In these systems, with increasing temperature, the continuous tetrahedral network of hydrogen bonds is destroyed (at 373 K), and in the more concentrated solution this network is absent even at the standard temperature. The hydrogen bonding of the solvent molecules in the LiBr:15H<sub>2</sub>O and

LiBr:8H<sub>2</sub>O systems is preserved on heating, although the number of H bonds appreciably decreases.

Heating considerably weakens the coordinative power of the Li<sup>+</sup> ion and hence decreases the degree of ordering of water molecules in its first hydration sphere; this influence of temperature is stronger in more concentrated solutions. The coordinative power of the anion is affected by temperature insignificantly. In all the three systems, heating causes considerable decrease in the number of Br<sup>−</sup>⋯H bonds, which illustrates extensive rupture of hydrogen bonds between the anion and water molecules of its first hydration sphere.

As the temperature grows, the amount of contact ion pairs in the LiBr:15H<sub>2</sub>O and LiBr:8H<sub>2</sub>O solutions considerably increases, and that of hydration-separated ion pairs decreases, with the first trend being more pronounced.

Isobaric heating affects the structuring of the LiBr:4H<sub>2</sub>O solution peculiarly. In this system, the tetrahedral network of water molecules is absent even at standard temperature. The number of O–H bonds is considerably smaller, and the amount of contact ion pairs, larger than in the less concentrated systems. In contrast to the less concentrated solutions, the number of O–H bonds and the amount of hydration-separated ion pairs in this system increase with heating. Presumably, such properties of the highly concentrated LiBr solution are caused by formation of a melt-like bond system.

## ACKNOWLEDGMENTS

The study was financially supported by the Russian Foundation for Basic Research (project no. 01-03-32278).

## REFERENCES

1. Nakahara, M., Yamaguchi, T., and Ohtaki, H., *Recent Res. Devel. Phys. Chem.*, 1997, vol. 1, p. 17.
2. Nakahara, M. and Wakai, C., *J. Mol. Liq.*, 1995, vol. 65/66, p. 149.
3. Yamanaka, K., Yamaguchi, T., and Wakita, H., *J. Chem. Phys.*, 1994, vol. 101, no. 11, p. 9830.
4. Radnai, T. and Ohtaki, H., *Mol. Phys.*, 1986, vol. 87, no. 1, p. 103.
5. Tromp, R.H., Postorino, P., Neilson, G.W., Ricci, M.A., and Soper, A.K., *J. Chem. Phys.*, 1994, vol. 101, no. 9, p. 6210.
6. Cummings, P.T., Cochran, H.D., Simonson, J.M., Mesmer, R.E., and Karaborni, N.J., *J. Chem. Phys.*, 1991, vol. 94, no. 8, p. 5606.

7. Kalinichev, A.G. and Bass, T.D., *J. Phys. Chem.*, 1997, vol. 101, no. 50, p. 9720.
8. Kataoka, Y., *J. Chem. Phys.*, 1989, vol. 90, no. 3, p. 1866.
9. Jedlovsky, P. and Richardi, J., *J. Chem. Phys.*, 1999, vol. 110, no. 16, p. 8019.
10. Krishtal, S., Kiselev, M., Puhovski, Y., Kerdcharoen, T., Hannongbua, S., and Heinzinger, K., *Z. Naturforsch. (a)*, 2001, vol. 56, p. 579.
11. Gorbatiy, Yu.E. and Dem'yanets, Yu.N., *Dokl. Akad. Nauk SSSR*, 1981, vol. 260, no. 4, p. 911; *Dokl. Akad. Nauk SSSR*, 1984, vol. 275, no. 4, p. 903; *Zh. Strukt. Khim.*, 1982, vol. 23, no. 6, p. 73; *Zh. Strukt. Khim.*, 1983, vol. 24, no. 3, p. 66.
12. Chialvo, A.A. and Cummings, P.T., *Adv. Chem. Phys.*, 1999, vol. 109, p. 115.
13. Soper, A.K., *Chem. Phys.*, 2000, vol. 258, no. 2/3, p. 121.
14. Ohtaki, H., Radnai, T., and Yamaguchi, T., *Chem. Soc. Rev.*, 1997, vol. 26, no. 1, p. 41.
15. Balbuena, P.B., Johnston, K.P., and Rossky, P.J., *J. Phys. Chem.*, 1996, vol. 100, no. 7, p. 2716.
16. De Jong, P.H.K. and Neilson, G.W., *J. Chem. Phys.*, 1997, vol. 107, no. 14, p. 8577.
17. Yamaguchi, T., Yamagami, M., Ohzono, H., Yamana, K., and Wakita, H., *Physica (B)*, 1995, vols. 213–214, no. 4, p. 480.
18. Nishikawa, K. and Morita, T., *J. Supercrit. Fluids*, 1998, vol. 13, p. 143.
19. Flanagan, L.W., Balbuena, P.B., Johnston, K.P., and Rossky, P.J., *J. Phys. Chem.*, 1995, vol. 99, no. 14, p. 5196.
20. Chialvo, A.A., Cummings, P.T., Simonson, J.M., and Mesmer, R.E., *Fluid Phase Equil.*, 1998, vols. 150–151, p. 107.
21. Cui, S.T. and Harris, J.G., *Chem. Eng. Sci.*, 1994, vol. 49, no. 17, p. 2749.
22. Reagan, M.T., Harris, J.G., and Tester, J.W., *J. Phys. Chem. (B)*, 1999, vol. 103, no. 37, p. 7935.
23. Hummer, G., Soumpasis, D., and Neumann, M., *Mol. Phys.*, 1992, vol. 77, no. 4, p. 769; *Mol. Phys.*, 1994, vol. 81, no. 5, p. 1155.
24. Holovko, M.F., Kalyuzhny, Yu.V., and Heinzinger, K., *Z. Naturforsch. (a)*, 1990, vol. 54, p. 687.
25. Chialvo, A.A., Kusalik, P.G., Kalyuzhny, Yu.V., and Cummings, P.T., *J. Stat. Phys.*, 2000, vol. 100, no. 1/2, p. 167; *J. Chem. Phys.*, 2001, vol. 114, no. 8, p. 3575.
26. Oparin, R.D., Fedotova, M.V., and Trostin, V.N., *Zh. Obshch. Khim.*, 1998, vol. 68, no. 10, p. 1625.
27. Oparin, R.D., Fedotova, M.V., and Trostin, V.N., *Izv. Ross. Akad. Nauk, Ser. Khim.*, 2001, no. 6, p. 897.
28. Fedotova, M.V. and Trostin, V.N., *Zh. Fiz. Khim.*, 1999, vol. 73, no. 6, p. 1025.
29. Oparin, R.D., Fedotova, M.V., and Trostin, V.N., *Zh. Obshch. Khim.*, 2000, vol. 70, no. 11, p. 1779.
30. Oparin, R.D., Fedotova, M.V., and Trostin, V.N., *Zh. Fiz. Khim.*, 2001, vol. 75, no. 5, p. 873.
31. Fedotova, M.V., Oparin, R.D., and Trostin, V.N., *J. Mol. Liq.*, 2001, vol. 91, p. 123.
32. Fedotova, M.V., Oparin, R.D., and Trostin, V.N., *Zh. Strukt. Khim.*, 2002, vol. 43, no. 3, p. 511.
33. Chandler, D. and Andersen, H.C., *J. Chem. Phys.*, 1972, vol. 57, no. 5, p. 1930.
34. Berendsen, H.J.C., Postma, J.P.M., Gunsteren, W.F. van, and Hermans, J., *Abstracts of Papers, Jerusalem Symp. on Quantum Chemistry and Biochemistry*, Pullman, B., Ed., Dordrecht: Reidel, 1981, p. 331.
35. Pettitt, B.M. and Rossky, P.J., *J. Chem. Phys.*, 1982, vol. 77, no. 3, p. 1451.
36. Lee, S.H. and Rasaiah, J.C., *J. Phys. Chem.*, 1996, vol. 100, no. 4, p. 1420.
37. Fumi, F.G. and Tosi, M.P., *J. Phys. Chem. Solids*, 1964, vol. 25, no. 1, p. 31.
38. Kalyuzhnyi, Yu.V., Fedotova, M.V., Golovko, M.F., and Trostin, V.N., *Preprint of the Inst. of Physics of Condensed Systems, Ukrainian Acad. Sci.*, Lviv, 1994, no. IFKS-93-27R.
39. Narten, A.H., X-ray Diffraction Data on Liquid Water in the Temperature Range 4–200°C, *ORNL-4578*, Oak Ridge, 1970.
40. Levy, H.A., Danford, M.D., and Narten, A.H., *Data Collection and Evolution with an X-ray Diffractometer Designed for the Study of Liquid Structure*, *ORNL-3960*, Oak Ridge, 1966.
41. Narten, A.H., Danford, M.D., and Levy, H.A., X-ray Diffraction Data on Liquid Water in the Temperature Range 4–200°C, *ORNL-3997*, Oak Ridge, 1966.
42. Palinkas, G., Kalman, E., and Kovacs, P., *Mol. Phys.*, 1977, vol. 34, p. 525.
43. Valyashko, V.M., *Fazovye ravnovesiya i svoystva gidrotermal'nykh sistem* (Phase Equilibria and Properties of Hydrothermal Systems), Moscow: Nauka, 1990.
44. Gorbatiy, Yu.E. and Demianets, Yu.N., *Mol. Phys.*, 1985, vol. 55, no. 3, p. 571; *Chem. Phys. Lett.*, 1983, vol. 100, no. 5, p. 450.
45. Lindner, H.A., *Dissertation*, Univ. Karlsruhe (FRG), 1970.
46. Kataoka, Y., *Bull. Chem. Soc. Jpn.*, 1989, vol. 62, no. 5, p. 1421.

47. Narten, A.H., Vaslow, F., and Levy, H.A., *J. Chem. Phys.*, 1973, vol. 58, no. 11, p. 5017.
48. Palinkas, G., Radnai, T., and Hajdu, F., *Z. Naturforsch. (a)*, 1980, vol. 35, p. 107.
49. Paschina, G., Piccaluga, G., Pinna, G., and Magini, M., *Chem. Phys. Lett.*, 1983, vol. 98, no. 2, p. 157.
50. Ohtomo, N. and Arakawa, K., *Bull. Chem. Soc. Jpn.*, 1979, vol. 52, no. 10, p. 2755.
51. Takamuku, T., Yamagami, M., Wakita, H., and Yamaguchi, T., *Z. Naturforsch. (a)*, 1997, vol. 52, p. 521.
52. Licheri, G., Piccaluga, G., and Pinna, G., *J. Chem. Phys.*, 1975, vol. 63, p. 4412.
53. Licheri, G., Piccaluga, G., and Pinna, G., *Chem. Phys. Lett.*, 1975, vol. 35, no. 1, p. 119.
54. Licheri, G., Piccaluga, G., and Pinna, G., *J. Appl. Crystallogr.*, 1973, vol. 6, no. 2, p. 392.
55. Lawrence, R.M. and Kruh, R.F., *J. Chem. Phys.*, 1967, vol. 47, no. 8, p. 4758.
56. Valyashko, V.M., *Probl. Sovrem. Khim. Koord. Soedin.*, 1993, no. 11, p. 75.